

Quarantines as a Targeted Immunization Strategy

JESSICA HOFFMANN* and MATT JORDAN*, The University of Texas at Austin
 CONSTANTINE CARAMANIS, The University of Texas at Austin

In the context of the recent COVID-19 outbreak, quarantine has been used to “flatten the curve” and slow the spread of the disease. In this paper, we show that this is not the only benefit of quarantine for the mitigation of an SIR epidemic spreading on a graph. Indeed, human contact networks exhibit a powerlaw structure, which means immunizing nodes at random is extremely ineffective at slowing the epidemic, while immunizing high-degree nodes can efficiently guarantee herd immunity. We theoretically prove that if quarantines are declared at the right moment, high-degree nodes are disproportionately in the Removed state, which is a form of targeted immunization. Even if quarantines are declared too early, subsequent waves of infection spread slower than the first waves. This leads us to propose an opening and closing strategy aiming at immunizing the graph while infecting the minimum number of individuals, guaranteeing the population is now robust to future infections. To the best of our knowledge, this is the only strategy that guarantees herd immunity without requiring vaccines. We extensively verify our results on simulated and real-life networks.

Additional Key Words and Phrases: epidemics, random graphs, networks, stochastic processes

ACM Reference Format:

Jessica Hoffmann, Matt Jordan, and Constantine Caramanis. 2021. Quarantines as a Targeted Immunization Strategy. *J. ACM* 37, 4, Article 111 (August 2021), 28 pages. <https://doi.org/10.1145/1122445.1122456>

1 INTRODUCTION

Most real-life networks, from the technological (the Internet [15, 44], train routes [70], electronic circuits [39]) to the biological (neural networks [81, 82], protein interaction networks [40]) exhibit a powerlaw structure. Human networks are no exception (the film actors network [7, 81], the telephone-call graph [3, 4], the sexual contact graph [49, 50]). Recent tracking studies have confirmed that the network of proximity contact follows the same distribution [41, 68].

When it comes to epidemics, this has terrible consequences. In particular, this means that the epidemic threshold is vanishing [62], which implies that measures to reduce the probability of infection (hand-washing, social distancing, etc.) can slow the spread of the disease, but not stop the outbreak. It also implies that an outbreak is likely to start anew even from a single infected individual (e.g. a traveler). Only measures that break the structure of the graph (such as quarantine, closing restaurants and parks, prohibiting groups of more than 10 etc.) can stop the spread. Moreover, powerlaw graphs are incredibly resistant to *random* failures [6], which means that removing individuals at random (for instance if they received a vaccine, or if they caught the disease and developed immunity) will not change these properties. As most countries affected by COVID-19

*Both authors contributed equally to this research.

Authors’ addresses: Jessica Hoffmann, hoffmann@cs.utexas.edu; Matt Jordan, mjordan@cs.utexas.edu, The University of Texas at Austin; Constantine Caramanis, The University of Texas at Austin, constantine@utexas.edu.

Permission to make digital or hard copies of all or part of this work for personal or classroom use is granted without fee provided that copies are not made or distributed for profit or commercial advantage and that copies bear this notice and the full citation on the first page. Copyrights for components of this work owned by others than ACM must be honored. Abstracting with credit is permitted. To copy otherwise, or republish, to post on servers or to redistribute to lists, requires prior specific permission and/or a fee. Request permissions from permissions@acm.org.

© 2021 Association for Computing Machinery.

0004-5411/2021/8-ART111 \$15.00

<https://doi.org/10.1145/1122445.1122456>

are relaxing quarantine while many infected individuals remain infected, one might think that the second wave will be identical to the first wave.

However, if powerlaw graphs are resistant to random failure, they are very susceptible to targeted immunization [6]. As shown in the previously mentioned paper, vaccinating only a small percentage of the nodes of the graph (the nodes of highest degree) is enough to achieve herd immunity, while it is never achievable with random immunization. The key observation here is that epidemic spread is *not* equivalent to random immunization. In particular, nodes of high degree get infected much more quickly than nodes of low degree [62]. If we let the epidemic run its course, this superspreader phenomenon would just help the epidemic spread rapidly to all the nodes in the network. However, if the epidemic is temporarily halted, say because of a mandatory quarantine, in the SIR model this implies that nodes of high degree will become immunized without having had the possibility of spreading the infection. Multiple quarantines can then become an ersatz to achieving herd immunity (or at least slow its spread and "flatten the curve") before a vaccine is developed.

Note that if we let the disease spread and infect the entire population, we would technically achieve herd immunity. Our goal is then to balance how many people get infected while guaranteeing the population gets immunized. Leveraging results from random graphs analysis and percolation theory, we theoretically show that even a *single* well-timed quarantine can be used to achieve herd immunity and significantly reduce the fraction of the infected population.

1.1 Relevant work

The study of epidemics on graphs is an active field of research. An important body of work assumes the underlying graph is known, and focuses on modeling epidemics [17, 20, 33, 51, 83, 86], detecting whether there is an epidemic [8, 9, 42, 47, 56, 58, 59], finding communities [65, 84], localizing the source of the spread [21, 71–73, 76, 77, 80] or instead obfuscating it [27–29], or controlling their spread [22, 23, 30, 35, 45, 63, 79, 85]. The inverse problem, recovering the network from epidemic data, has also been extensively studied [1, 19, 34, 36, 43, 61, 64].

This paper is interested in immunization strategies. [6] already showed that immunizing about 3% of the nodes of highest degree is enough to reach herd immunity for any powerlaw graph, no matter the exponent. [18] proposed a local strategy in case the global structure of the graph is unknown: we pick a fraction ρ of the population; each of those individuals then names someone they personally know. It turns out that the person selected has a higher chance of being well-connected than the person who nominated them, following the well-known principle stating that "your friends have more friends than you." This paper relies on a similar idea: someone infecting someone else is similar to someone nominating someone else, which explains why nodes of highest degree get infected faster. Other immunization strategies have been proposed [13, 16, 37, 69].

Many scientists have joined the fight against COVID-19, and work has been done to predict the evolution of the epidemic [12, 24, 32, 74], predict diagnostics [2, 75], analyze the spread of misinformation about the pandemic online [5, 60], design tracking algorithms and technologies [11, 14, 53], analyze testing and interventions policies [25, 26, 52, 54], and more. One other work [31] has analyzed quarantine strategies, albeit without taking into consideration the impact on the graph, which is our main contribution. This work aims to analyze quarantines and emphasize their impact as a targeted immunization strategy, which would be robust to future reinfections (contrary to contact tracing strategies, for instance).

1.2 Main contributions

The contributions of this paper are as follows:

- While quarantines have been introduced to slow the spread of COVID-19, we show that they transform the structure of the human contact graph, and negatively impact the diffusion of the disease during the subsequent waves.
- We characterize when to declare the quarantine in order to achieve herd immunity. For simple powerlaw graph of exponent 3 in the configuration model, this corresponds to when about 8% of the graph is infected.
- While the number above is higher than what we would hope, it is important to note that after this single quarantine, outbreaks cannot start again from a constant number of individuals. As such, this is the first long-term immunization solution which is robust to reinfections but does not require a vaccine.
- If we have some limitations on the maximum number of infected individuals (*e.g.* a limited number of hospital beds), we experimentally show that we can declare multiple quarantines and recover the result from a single quarantine.
- We experimentally confirm our results on a wide range of simulated and real-life networks. While our theoretical results are proven on a specific random graph model, we experimentally show that relaxing the theoretical assumptions we require in our proofs (infinite graph, vanishing clustering coefficient, etc.) does not qualitatively impact the results. In particular, well-timed quarantines are a valid targeted immunization strategy for real-life networks.

2 PRELIMINARIES

2.1 Notations

The epidemic spreads on a (possibly infinite) directed graph $G = (V, E)$, where V is the set of nodes and E the set of edges. If $|V| < \infty$, we write $|V| = N$. When considering a random graph drawn from a specific distribution \mathcal{D} , we denote by P_k the random variable representing the number of nodes of degree k in the graph, p_k the fraction of nodes of degree k , $\langle k \rangle$ the average degree given the graph, and q_k the fraction of nodes of excess degree k , defined by $q_k = \frac{(k+1)p_k}{\langle k \rangle}$. As a shorthand, we write $\mathbb{E}_{\{L_k\}_{k=0}^{\infty}} [k] = \sum_{k=0}^{\infty} L_k \cdot k$. If no sequence $\{L_k\}_{k=0}^{\infty}$ is specified, we assume $L_k = P_k$, and $\mathbb{E}[k] = \langle k \rangle$ and $\mathbb{E}[k^2]$ represent the average degree and degree squared given the graph. Throughout the paper, we use the following functions:

DEFINITION 1 (GENERATIVE FUNCTION). *For a given graph, the generative function of the degrees g_0 and excess degrees g_1 are defined as:*

$$g_0(z) = \mathbb{E}_{\{p_k\}_{k=1}^{\infty}} [z^k] = \sum_{k=1}^{\infty} p_k \cdot z^k,$$

$$g_1(z) = \mathbb{E}_{\{q_k\}_{k=1}^{\infty}} [z^k] = \sum_{k=1}^{\infty} q_k \cdot z^k = \frac{g_0'(z)}{\langle k \rangle}.$$

2.2 Model

SIR model on graphs: We consider the spread of a Susceptible \rightarrow Infected \rightarrow Removed (SIR) epidemic on a directed graph $G = (V, E)$, possibly infinite. Each node belongs to one of these three states. Infected nodes can infect the susceptible nodes with which they share an edge, also called their *neighbors* in the graph. Each infection along an edge is independent of other infections. Infected nodes spontaneously transition to the Removed state after a non-deterministic time. Once in the Removed state, nodes do not interact with the epidemic anymore.

Spreading model: The results presented in this paper are spreading-mechanism agnostic. Our theoretical results do not rely on restrictions on the spreading process. While our experiments are shown on classical continuous-time SIR spread, we do not believe the spreading process would change the outcome.

Configuration model: Our theoretical results are established in the configuration model [62], an established setting to study random graphs. In this model, we specify the number of nodes P_k of degree k . We assume the sum of all P_k is even. We then assign stubs to nodes, such that the number of nodes with k stubs is exactly P_k . Following this, we pick two stubs at random, and connect them. We repeat the process until no stubs are left. We say the resulting graph was drawn from the configuration model with degrees sequence $\{P_k\}_{k=0}^{\infty}$.

Powerlaw graphs: We emphasize the results on powerlaw graphs. A powerlaw graph of exponent α is a random graph with degree distribution following the law $p_k \sim \frac{C}{k^\alpha}$.

Simple powerlaw graphs: We say a graph is a simple powerlaw graph of exponent α if its distribution follows exactly $p_k = \frac{1}{\zeta(\alpha)} \frac{1}{k^\alpha}$ for $k \geq 1$, $\alpha > 1$.

Barabási–Albert (BA) graph: A Barabási–Albert (BA) graph of parameter m is constructed by adding nodes one by one, each new node attaching m new edges to previous nodes, picking the node to attach to at random with probability proportional to the degree of the previous nodes (preferential attachment). These graphs follow the configuration model by construction. In expectation, these graphs have powerlaw distribution with exponent 3, with exact degree distribution given by $p_k = \frac{2m(m+1)}{k(k+1)(k+2)} \sim \frac{C}{k^3}$ for $k \geq m$.

2.3 Known results in the configuration model

We recall known results in the configuration model, which we use in the rest of our proofs.

CLAIM 1 (EXPONENTIAL GROWTH, PROVED IN [62]). *In the configuration model, the reproductive number $R = \frac{c_2}{c_1}$, which represents the number of 2nd neighbors divided by the number of 1st neighbors, can be computed from the sequence of degrees $\{P_k\}_{k=0}^N$. Its value is:*

$$R = \frac{\mathbb{E}[k^2] - \mathbb{E}[k]}{\mathbb{E}[k]}.$$

CLAIM 2 (HERD IMMUNITY, PROVED IN [62]). *In the configuration model, an outbreak is possible if and only if $R > 1$, or equivalently:*

$$\mathbb{E}[k^2] - 2\mathbb{E}[k] > 0.$$

If the above equation is not satisfied, we have achieved herd immunity.

LEMMA 1 (DISPARITY IN INFECTION RATE BY DEGREE, PROVED IN [62]). *In the configuration model, let $u(t)$ be the expected fraction of nodes of degree 1 in the susceptible state after time t . Then as a first order approximation, the expected fraction of nodes of degree k in the susceptible state is $u(t)^k$.*

Remark: The lemma above is an approximation. In particular, it takes into account how many nodes of degree k become Removed because they got infected, but not that the number of nodes of degree k decreases as their neighbors get infected (as their degree becomes lower than k) and increases whenever nodes of degree $k + c$ get c neighbors in the Removed state.

2.4 Known results for powerlaw graphs

We start by recalling the definition of epidemic thresholds:

DEFINITION 2 (EPIDEMIC THRESHOLD, PROVED IN [62]). *For SIR epidemics on graph, there exists a phase transition. If the parameters of the epidemic are above the epidemic threshold, outbreaks occur; otherwise, the epidemic dies out quickly. The closer we are to the epidemic threshold (from above), the smaller the outbreak is.*

The crucial result about human networks is that epidemic threshold for infinite powerlaw graphs is 0.

LEMMA 2 (VANISHING THRESHOLD, PROVED IN [62]). *Infinite powerlaw graphs with exponents between 2 and 3.4788 have a vanishing epidemic threshold.*

The higher the reproductive number R is compared to the epidemic threshold, the more likely an outbreak occurs, and the bigger its expected size is. When the epidemic threshold is 0, this means that changing the parameters of the spread (for instance by enforcing hand-washing or masks-wearing) can slow the spread of the disease and reduce the total number of infected people, but not prevent that there will be an outbreak. It also means that a single infected traveler can restart a major outbreak. In practice, real graphs are finite, which implies the epidemic threshold is bounded away from 0. However, the larger the graph, the lower the epidemic threshold.

CLAIM 3. *The generative function of the degrees g_0 and excess degrees g_1 for an infinite powerlaw graph of parameter α is given by:*

$$g_0(z) = \frac{1}{\zeta(\alpha)} \sum_{k=1}^{\infty} \frac{z^k}{k^\alpha} = \frac{Li_\alpha(z)}{\zeta(\alpha)}$$

$$g_1(z) = \frac{1}{\zeta(\alpha-1)} \sum_{k=1}^{\infty} \frac{z^{k-1}}{k^{\alpha-1}} = \frac{Li_{\alpha-1}(z)}{z \cdot \zeta(\alpha-1)}$$

3 ONE QUARANTINE

In this section, we prove our main result, which is that for certain types of graphs, it is possible to achieve herd immunity by timing a *single* quarantine adequately. We therefore study the effect of quarantine timing on the structure of the graph. We are particularly interested in whether it is possible to achieve herd immunity, and how to minimize the total number of people who have been touched by the epidemic. For the remainder of the paper, we study perfect quarantines, as defined below:

DEFINITION 3 (QUARANTINE). *We call perfect quarantine (henceforth just quarantine) the complete halt of the spread of the epidemic. During a quarantine, all Infected nodes transition to the Removed state, and no new nodes become Infected.*

3.1 The quarantine operator

In the configuration model, the expected behavior of the spread of epidemics is governed by the sequences of degrees $\{P_k\}_{k=0}^{N-1}$. We start by studying the impact of a quarantine on that sequence of degrees.

LEMMA 3. *Let $u(t)$ be the fraction of nodes of degree 1 that are susceptible after letting the epidemic spread for time t . Suppose we declare a quarantine when $u(t)$ reaches the value u . Let $T_Q : \mathbb{N}^N \rightarrow \mathbb{R}^N$ be the operator representing the transformation of the expected number of susceptible nodes after one iteration of letting the epidemic grow, then declaring a quarantine. Then:*

$$T_Q(\{P_k\}_{k=0}^{N-1}) = \{P_k \cdot u^k\}_{k=0}^{N-1}.$$

PROOF. This is a direct implication of Lemma 1 from the Preliminaries.

As it turns out, the number of nodes in the Removed state can be computed easily from the above result.

CLAIM 4. Let $g_0(z)$ be the generative function of the distribution of degrees. The expected fraction of nodes in the Removed state after one quarantine R_Q is:

$$R_Q = 1 - g_0(u).$$

PROOF. Let p_k be the fraction of nodes of degrees k in the graph, so that $P_k = N \cdot p_k$. Notice that for $k \geq N$, there exist no nodes of that degree, so $p_k = 0$. The generative function of the distribution of degrees is $g_0(z) = \sum_{j=0}^{\infty} p_j z^j$.

$$\begin{aligned} R_Q &= \frac{1}{N} \left(N - \sum_{j=0}^N T_Q(\{P_k\}_{k=0}^N)_j \right) \\ &= \frac{1}{N} \left(N - \sum_{j=0}^N P_j \cdot u^j \right) \\ &= 1 - \sum_{j=0}^{\infty} p_j \cdot u^j \\ &= 1 - g_0(u). \end{aligned}$$

3.2 Achieving herd immunity

3.2.1 *General graphs.* It is possible to give general results for any graph in the configuration model, which we do in this section.

CLAIM 5. Let u be the remaining fraction of susceptible nodes of degree 1 when we start the quarantine. We achieve herd immunity for u such that:

$$u^2 g_0''(u) - u g_0'(u) \leq 0.$$

PROOF. Following Claim 2, we want to find u such that $\mathbb{E}_{T_Q}[k^2] - 2\mathbb{E}_{T_Q}[k] \leq 0$. This translates to:

$$\begin{aligned} \mathbb{E}_{T_Q}[k^2] - 2\mathbb{E}_{T_Q}[k] &= \sum_{k=0}^{\infty} P_k \cdot u^k k^2 - 2 \sum_{k=0}^{\infty} P_k \cdot u^k k \\ &= \sum_{k=0}^{\infty} P_k \cdot u^k k^2 - \sum_{k=0}^{\infty} P_k \cdot u^k k - \sum_{k=0}^{\infty} P_k \cdot u^k k \\ &= \sum_{k=0}^{\infty} P_k \cdot u^k k(k-1) - \sum_{k=0}^{\infty} P_k \cdot u^k k \\ &= u^2 g_0''(u) - u g_0'(u) \\ &\leq 0. \end{aligned}$$

However, further analysis requires better knowledge of the network topology. We now focus on specific types of random graphs.

3.2.2 Simple powerlaw graphs. Here, we provide our first numerical results for simple powerlaw graphs, and show that well-timed quarantine can guarantee herd immunity while drastically reducing the fraction of Infected nodes.

CLAIM 6. *Let u be the remaining fraction of susceptible nodes of degree 1 when we start the quarantine. For an infinite simple powerlaw graph of exponent 3, we achieve herd immunity for $u \leq 0.940599$.*

PROOF. We want to find u such that:

$$\begin{aligned} \mathbb{E}_{T_Q}[k^2] - 2\mathbb{E}_{T_Q}[k] &= \sum_{k=1}^{\infty} \frac{C}{k^3} \cdot u^k k^2 - 2 \sum_{k=1}^{\infty} \frac{C}{k^3} \cdot u^k k \\ &= C \sum_{k=1}^{\infty} \frac{u^k}{k} - 2 \frac{u^k}{k^2} \\ &= -C \cdot (2Li_2(u) - \log(1 - u)) \\ &\leq 0. \end{aligned}$$

Where $Li_2(u)$ is the polylog-2 function. Solving this equation numerically yields $u \leq 0.940599$.

We now look at the total number of nodes in the Removed state in this case:

CLAIM 7. *For a simple infinite powerlaw graph of exponent 3, if we declare a quarantine when a fraction $u' = 0.940599$ of nodes of degree 1 are still in the susceptible state, then by the end of quarantine, at least $R_Q = 92.2912\%$ of the nodes are still in the susceptible state.*

PROOF. Remembering that $C = \frac{1}{\zeta(3)}$, where $\zeta(x) = \sum_{k=1}^{\infty} \frac{1}{k^x}$, the number of susceptible nodes is:

$$g_0(u') \geq \frac{1}{\zeta(3)} \sum_{k=1}^N \frac{u'^k}{k^3} \approx 0.922912.$$

Combining Claims 6 and 7, the network can therefore achieve herd immunity while infecting a bit less than 8% of the nodes:

THEOREM 1. *For simple infinite powerlaw graphs of exponent 3, min-degree 1, it is possible to achieve herd immunity by declaring a single quarantine when a bit less than 6% of the nodes of degree 1 are Infected. In this case, less than 8% of the nodes will be Removed at the end of the quarantine.*

Remarks:

- Far from only "flattening the curve", quarantines can be used to achieve herd immunity.
- The result above is both positive (only 8% of Removed nodes) and disappointing: this is the best achievable, in the sense that nothing else we can do in this optimistic quarantine model can reduce the fraction of Removed nodes at the end. In most cases, 8% of the population being Infected represents millions of people, and is not desirable. In the case of COVID-19, however, the fraction of Infected people has passed this number in a number of countries.
- The result above is valid for simple powerlaw graph. The exact percentage varies widely with the type of powerlaw graph, as we see below, and in section 4.

3.2.3 Barabási–Albert (BA) graphs. BA graphs are a well-known family of random powerlaw graphs. We show below that quarantine-based immunization strategies require a higher number of Removed nodes by the time we achieve herd immunity than simple powerlaw graphs (despite having the same min-degree). The exact value of the gain depends on the sequence of degrees $\{P_k\}_{k=0}^{N-1}$, but the qualitative behavior remains the same.

CLAIM 8. *Let u be the remaining fraction of susceptible nodes of degree 1 when we start the quarantine. For a Barabási–Albert (BA) of parameter $m = 1$, we achieve herd immunity if we declare a quarantine when:*

$$u^2 - 4u + 3u \log(1 - u) - 4 \log(1 - u) \leq 0.$$

Solving numerically, we obtain $u \leq 0.776621$.

PROOF. Let $g_0(u) = \sum_{k=m}^{\infty} p_k u^k$ be the probability generative function of a BA graph of parameter $m = 1$. We know $p_k = \frac{2m(m+1)}{k(k+1)(k+2)} = \frac{4}{k(k+1)(k+2)}$. Using Claim 5, we have:

$$\begin{aligned} u^2 g_0''(u) - u g_0'(u) &= u^2 \sum_{k=1}^{\infty} \frac{4(k-1)}{(k+1)(k+2)} u^{k-2} - u \sum_{k=1}^{\infty} \frac{4}{(k+1)(k+2)} u^{k-1} \\ &= \sum_{k=1}^{\infty} \frac{4(k-2)}{(k+1)(k+2)} u^k \\ &= 4 \frac{u^2 - 4u + 3u \log(1 - u) - 4 \log(1 - u)}{u^2}. \end{aligned}$$

Since we need $u^2 g_0''(u) - u g_0'(u) \leq 0$ according to Claim 5, this is equivalent to $u^2 - 4u + 3u \log(1 - u) - 4 \log(1 - u) \leq 0$. Numerically, we obtain $0 \leq u \leq 0.776621$.

THEOREM 2. *For a BA graphs of parameter $m = 1$, it is possible to achieve herd immunity by declaring a single quarantine when a bit less than 23% of the nodes of degree 1 are Infected. In this case, less than 33% of the nodes will be Removed at the end of the quarantine.*

3.2.4 Non-powerlaw graphs. The fact that quarantines can be used as a targeted immunization strategy is a direct result of the heavy-tail distribution of human networks. Here, we illustrate that if contact networks had a different graph structure, we could not achieve herd immunity using a well-timed quarantine without infecting most of the graph – if not the entire graph. We prove this for Poisson graphs, which do have a tail, albeit lighter than powerlaw graphs, and d -regular graphs, which do not have a tail.

PROPOSITION 3. *For Poisson graphs of parameter λ in the configuration model, i.e. with $p_k = \frac{\lambda^k e^{-\lambda}}{k!}$ for $k \geq 0$, it is possible to achieve herd immunity after one quarantine. To compare with BA graphs of parameter $m = 1$, we pick $\lambda = 2$, so that both graphs will have same average degree. In this case, a bit more than 63% of nodes will be in the Removed state when herd immunity is achieved.*

PROOF. For Poisson graphs in the configuration model, we have:

$$\begin{aligned} g_0(x) &= \sum_{k=0}^{\infty} \frac{\lambda^k e^{-\lambda}}{k!} x^k \\ &= e^{\lambda x - \lambda}. \end{aligned}$$

Using Claim 5, we need to declare a quarantine when the fraction of nodes of degree 1 u is such that:

$$\begin{aligned} 0 &\geq u^2 g_0''(u) - u g_0'(u) \\ &= u^2 \lambda^2 e^{\lambda x - \lambda} - u \lambda e^{\lambda x - \lambda} \\ &= u \lambda (u \lambda - 1) e^{\lambda x - \lambda}. \end{aligned}$$

The epidemic threshold is therefore achieved after one quarantine declared when $u = \frac{1}{\lambda}$. In this case, the total number of nodes in the Removed state at the end of the infection is, in expectation, $1 - e^{\lambda \frac{1}{\lambda} - \lambda} = 1 - e^{1 - \lambda}$. When $\lambda = 2$, we obtain $1 - \frac{1}{e} \approx 63.2121\%$. \square

While the tail of Poisson graphs is not as heavy as powerlaw graph, it is still possible to achieve herd immunity, albeit at the cost of infecting a larger fraction of the population. For random d -regular graphs, however, it is impossible to use quarantines as a targeted immunization strategy:

PROPOSITION 4. *For random d -regular graphs in the configuration model, i.e. with $p_d = 1$ and for $k \neq d, p_k = 0$, it is possible to achieve herd immunity after one quarantine for $d > 2$.*

PROOF. See Appendix.

3.2.5 Summary. We summarize the results above in Table 1. We notice that experimental value are always below our theoretical predictions. As expected, on powerlaw graphs, Quarantine/Experiments-Q perform worse than High-degree, but significantly better than Random, although they do not require any vaccines. For graphs with lighter tail however, Random performs better. Using quarantine as a targeted immunization strategy is therefore only possible thanks to the very specific distribution of human networks.

Graph	Random	Quarantine	Experiments-Q	High-degree
Simple powerlaw/ $\alpha = 3, k_{min} = 1$	2%	8%	2%	3%
Barabási-Albert/ $\alpha = 3, m = 1$	47%	33 %	22%	1%
Poisson/ $\lambda = 2$	44%	65%	42%	9%
4-regular	64%	–	89%	64%

Table 1. We show immunization strategies on multiple network topologies: two powerlaw graphs (heavy-tail), a Poisson graph (lighter tail) and a d -regular graph (no tail). The number represent the number of nodes we need to immunize, either by vaccinating them (for Random and High-degree) or by just letting the epidemic spread (for Quarantine). In the Random strategy, we immunize nodes at random. In the High-degree strategy, we immunize nodes by decreasing values of degree. The Quarantine column represents our theoretical predictions, and Experiments-Q the values observed experimentally.

3.3 Minimizing the final number of Removed nodes

Below the epidemic threshold, the expected fraction of the population in the Removed state by the end of the epidemic is 0. However, above the epidemic threshold, not all nodes may become Infected by the end of the outbreak, and outbreaks tend to be of small size just above the epidemic threshold. Instead of timing quarantines to reach herd immunity, we might instead allow small outbreaks after our quarantine, provided that it reduces the final number of nodes in the Removed state. In this section, we study how to minimize this final number of Removed nodes, even if that means no reaching herd immunity.

In general, the expected total number of nodes in the Removed state at the end of an epidemic is in general given by:

CLAIM 9 (FROM NEWMAN [62]). *Let ϕ be the probability that an Infected node infects its susceptible neighbor, and g_0 be the generative function of the degrees of the nodes in the graph, and g_1 the generative function of the excess degrees. Then the expected number of Removed nodes at the end of the epidemic S is given by:*

$$S = 1 - g_0(v),$$

where v is the solution of the equation:

$$v = 1 - \phi + \phi g_1(v).$$

Notice that if $v = 1$, we are below the epidemic threshold, and $S = 0$. We can compute the generative functions of the degrees and the excess degrees of the graph after a quarantine has been declared:

CLAIM 10. *Let g_0^Q and g_1^Q be the generative functions of the degrees and the excess degrees of the resulting graph after a quarantine has been declared when a fraction u of the nodes of degree 1 remain susceptible. Then:*

$$\begin{aligned} g_0^Q(z) &= \frac{g_0(u \cdot z)}{g_0(u)}, \\ g_1^Q(z) &= \frac{g_1(u \cdot z)}{g_1(u)}. \end{aligned}$$

PROOF. Let p_k^Q and q_k^Q be the distribution of degrees and excess degrees after a quarantine. Using Claim 1, we know $p_k^Q = \frac{u^k \cdot p_k}{g_0(u)}$. Then:

$$\begin{aligned} g_0^Q(z) &= \sum_{k=0}^{\infty} p_k^Q z^k \\ &= \frac{1}{g_0(u)} \sum_{k=0}^{\infty} p_k \cdot (u \cdot z)^k \\ &= \frac{g_0(u \cdot z)}{g_0(u)}. \end{aligned}$$

Similarly, since $g_1(z) = \frac{g_0'(z)}{g_0'(1)}$, we have:

$$\begin{aligned} g_1^Q(z) &= \frac{g_0'^Q(z)}{g_0'^Q(1)} \\ &= \frac{u \frac{g_0'(u \cdot z)}{g_0(u)}}{u \frac{g_0'(u \cdot 1)}{g_0(u)}} \\ &= \frac{g_0'(u \cdot z)}{g_0'(u)} \\ &= \frac{g_0'(u \cdot z)}{g_0'(1)} \cdot \frac{g_0'(1)}{g_0'(u)} \\ &= \frac{g_1(u \cdot z)}{g_1(u)}. \end{aligned}$$

Now, it is possible to express the total number of Removed nodes $R(u)$ as a function of u , the fraction of susceptible nodes when we declare the quarantine:

LEMMA 4. *Suppose we declare a quarantine when a fraction u of nodes of degree 1 remain susceptible, then have an outbreak start again after the quarantine. The total expected fraction of Removed nodes $R(u)$ is given by:*

$$R(u) = 1 - g_0(u \cdot v),$$

with v solution of $v = 1 - \phi + \phi \frac{g_1(u \cdot v)}{g_1(u)}$.

PROOF. Let $R_{\text{beforeQ}}(u)$ be the number of Removed nodes at the end of a quarantine, and $R_{\text{afterQ}}(u)$ be the expected number of Removed nodes if an outbreak starts again after the quarantine. The total expected fraction of Removed nodes is given by $R(u) = R_{\text{beforeQ}}(u) + R_{\text{afterQ}}(u)$. We know, according to Claim 7, that:

$$R_{\text{beforeQ}}(u) = 1 - g_0(u).$$

We now position ourselves in the graph composed of only the nodes in the Susceptible state after the first quarantine. Notice that this graph is composed of a fraction $g_0(u)$ of the nodes of the original graph. According to Claims 9 and 10, we also have:

$$R_{\text{afterQ}}(u) = g_0(u) \cdot (1 - g_0^Q(v)) = g_0(u) \cdot \left(1 - \frac{g_0(u \cdot v)}{g_0(u)}\right) = g_0(u) - g_0(u \cdot v),$$

with v solution of $v = 1 - \phi + \phi g_1^Q(v) = 1 - \phi + \phi \frac{g_1(u \cdot v)}{g_1(u)}$.

Combining the two results, we get $R(u) = 1 - g_0(u) + g_0(u) - g_0(u \cdot v) = 1 - g_0(u \cdot v)$, which conclude the proof. \square

The equations above do not have closed form solutions in general, nor for powerlaw graphs in particular. However, we see in the experiment section below that $R(u)$ always seems to exhibit a V shape. If the expected size of an outbreak after a quarantine is very small, it might be better in term of the total number of Infected nodes to declare a quarantine early: letting the infection spread before a quarantine is declared (i.e. when the epidemic is probably in its exponential growth phase) would infect more nodes than having a small outbreak after the quarantine. Minimizing the total number of Infected nodes $R(u)$ is therefore related, but not equivalent to reaching herd immunity. We study $R(u)$ in more details in the next section.

4 EXPERIMENTS

The remainder of this paper focuses on empirical validation of our theoretical results on a variety of networks, both synthetically generated and taken from real world data sets. We begin by describing the networks examined and the simulation technique. Then we validate the major premise of this work: that higher degree nodes become Infected much more rapidly than lower degree nodes. Then we qualitatively and quantitatively describe the optimal time at which a single quarantine should be enacted, ablating on a variety of simulation parameters. Finally we discuss what is attainable in simulation when multiple quarantines are allowed.

4.1 Networks and Simulation Technique

Simulation setup: We first describe the simulation environment. All simulations are run using a continuous-time event-driven algorithm modeling an SIR infection [57]. The infection parameters are β and γ corresponding to the infection and recovery parameters respectively. We initialize an infection by uniformly randomly selecting ρ nodes to be Infected. When a quarantine is enacted,

every node in the Infected compartment is moved to the Removed compartment and we reinitialize the infection by randomly selecting ρ susceptible nodes to be Infected after the quarantine. As opposed to the previous section, in which quarantines were declared based on the fraction of Susceptible nodes of degree 1 remaining, here we declare quarantines based on the fraction of the general population that has already been Infected (i.e., in the Infected or Removed state, but not in the Susceptible state). We refer to a "quarantine threshold" as the fraction of the general population not in the Susceptible state when we declare the quarantine. All simulations are run until there are no more Infected nodes. Unless otherwise noted, we examine synthetic graphs with 10K nodes and set ρ to be equal to 10. By default, we set the recovery parameter γ to be 1 and primarily focus on the modest regime with infection parameter β as $\frac{1}{2}$. This places us in the regime where the infection typically spreads throughout the entire population, though we also ablate against varying ratios of $\frac{\beta}{\gamma}$.

Synthetic Networks: We run our simulations on a wide variety of synthetic networks. We describe these classes of networks here, briefly describing their structure and construction, and finally discuss a realistic choice for parameters.

The classical model proposed by Barabasi and Albert produces a graph with a power-law degree distribution with exponent 3 [10]. This model operates via an incremental growth mechanism leveraging preferential attachment: new nodes are added incrementally and connected to a fixed number m of existing nodes, where the probability of connection to a node is proportional to the degree of that node. There are two parameters of interest here: N , the number of nodes, and m , the number of edges added upon the inclusion of a new node. We refer to such graphs as **BA graphs**.

While BA graphs have, by design, scale-free degree distributions that emulate many real-world networks, they typically do not have the clustering behavior of real world networks. The clustering coefficient introduced by Watts and Strogatz quantifies this behavior as follows. The local clustering coefficient of node i in a network is defined as the number of edges contained within the neighborhood of node i , divided by the number of edges in a clique of the same size. The global clustering coefficient is the average local clustering coefficient over all nodes in the network. The Watts Strogatz network model generates a random graph with small average path lengths and more realistic clustering coefficients, however does not yield a graph with a scale-free degree distribution [81]. We refer to such graphs as **WS graphs**.

To rectify this situation and yield a network with a scale-free degree distribution and controllable clustering coefficients, Holme and Kim modified the BA network model [38]. This graph model, which we shall refer to as the power-law cluster, or **PLC**, model, follows the incremental growth and preferential attachment steps of the algorithm used to generate BA graphs, with one additional step: upon adding a new edge, say to node j , with a specified probability, a new edge is added to a neighbor of j . This network model has three parameters: N , the number of nodes; m , the number of edges added by the preferential attachment step; and p , the probability of adding a new edge to a neighbor. The clustering coefficient is controlled by the parameter p .

Similar to the PLC model is the random-walk model, **RW**, first introduced by Vázquez, which aims to generate a network in a method that emulates organic edge creation in a social network [78]. New nodes are added incrementally, where each node selects a random extant node to perform a random walk on. At each step, the random walk terminates with fixed probability, and each node in the random walk is connected to the new node with a fixed probability. This model generates networks with scale-free degree distributions and tunable clustering coefficients. The model has parameters: N , specifying the size of the graph; q_e , the probability of continuing the random walk; and q_v , the probability of adding an edge for each element of the random walk.

Net Type	Params	Deg	Cluster	Pathlength	Powerlaw Exp.
BA	($m = 5$)	9.99	0.007	3.66	2.94
BA	($m = 10$)	19.98	0.011	3.06	2.98
NN	($u = 0.88, k = 6$)	26.29	0.124	3.41	2.62
PLC	($m = 5, p = 0.5$)	9.99	0.178	3.53	2.67
PLC	($m = 10, p = 0.25$)	19.96	0.059	2.97	2.76
RW	($q_e = 0.91, q_v = 0.94$)	19.32	0.285	3.45	2.76
WS	($k = 10, p = 0.05$)	10	0.574	7.47	12.92

Table 2. Summary of Synthetic Networks considered. The parameters used for construction are provided, and summary statistics of the average degree, clustering coefficient, and average length of shortest path between two randomly selected nodes. We also use cumulative binning to estimate the powerlaw exponent for the degree distribution. All networks have 10k nodes. While these networks are randomly constructed, the summary statistics concentrate tightly around the reported values.

Finally, we consider the Nearest Neighbor model that emulates the behavior that two people with a mutual friend are more likely to become friends [78]. New nodes are connected to a random extant node and a random selection of 2-hop neighbors of the connected node. We use the modification where we also connect k pairs of random nodes upon addition of each graph. This process yields networks with scale-free degree distribution, and tunable clustering [67]. This model has parameters: N

Synthetic Network Parameter Selection: Each of the network models described above have at least one tunable parameter in addition to their parameter controlling network size. This begs the question of how these parameters should be chosen to emulate real-world social networks, such that a reasonable epidemic simulation may be performed. Fortunately, there is depth of prior work in fitting random network models to real world networks [55, 67]. We typically use the parameter as specified in [67] that have been fit to a region-based subnetwork from a private Facebook social graph. These parameters, as well as the average degree, clustering coefficient, and best-fit scale-free parameter are described in Table 2.

Real-world networks: We also perform simulations on three main classes of social networks. First we consider the large social network datasets on Facebook and Deezer, as presented in [66]. For Facebook, an edge denotes a mutual like for a verified facebook page of a particular category; for Deezer, edges are friendships. Next, we consider the Arxiv physics collaboration datasets taken from [46]. The data covers papers on Arxiv from the period of January 1993 and April 2003. Here nodes represent authors and a node exists between two authors if they appear on a paper together. All datasets were collected via SNAP [48].

4.2 Groupwise Survival Rates

We start with an experiment that motivates the premise of this work: higher degree nodes are more readily Infected, and lower-degree nodes survive much longer. This was shown in [62] in the configuration model, but we verify that it still applies even when the configuration model assumptions are violated (e.g. for real-life networks). As mentioned in 2.3, this behavior is an approximation. We verify the approximation holds for a real-world Facebook graph in Figure 1 (left). In this plot, we have grouped the 1,3,5% of nodes with highest degree and the nodes with the lowest degree, e.g. 10 for the BA graph with ($m = 10$). The vertical axis corresponds to the fraction of that group that resides in either the Infected or Removed compartment, and the horizontal axis corresponds to the fraction of the entire population in the Infected or Removed compartments. The

Net Type	Nodes	Deg	Cluster	Pathlength	Powerlaw Exp.
arxiv.AstroPh	18,770	21.11	0.631	4.19	2.83
arxiv.CondMat	23,131	8.08	0.633	5.36	3.11
arxiv.GrQc	5,240	5.53	0.53	6.05	2.88
arxiv.HepPh	12,006	19.74	0.611	4.67	2.31
arxiv.HepTh	9,875	5.26	0.471	5.94	3.28
deezer.HR	54,573	18.26	0.136	4.5	3.39
deezer.HU	47,538	9.38	0.116	5.34	3.79
deezer.RO	41,773	6.02	0.091	6.35	3.7
fb.artist	50,515	32.44	0.138	3.69	2.64
fb.athletes	13,866	12.53	0.276	4.28	2.85
fb.company	14,113	7.41	0.239	5.31	2.97
fb.government	7,057	25.35	0.411	3.78	2.58
fb.new_sites	27,917	14.78	0.295	4.39	2.85

Table 3. Summary of real networks used. The summary statistics are the same as in Table 2.

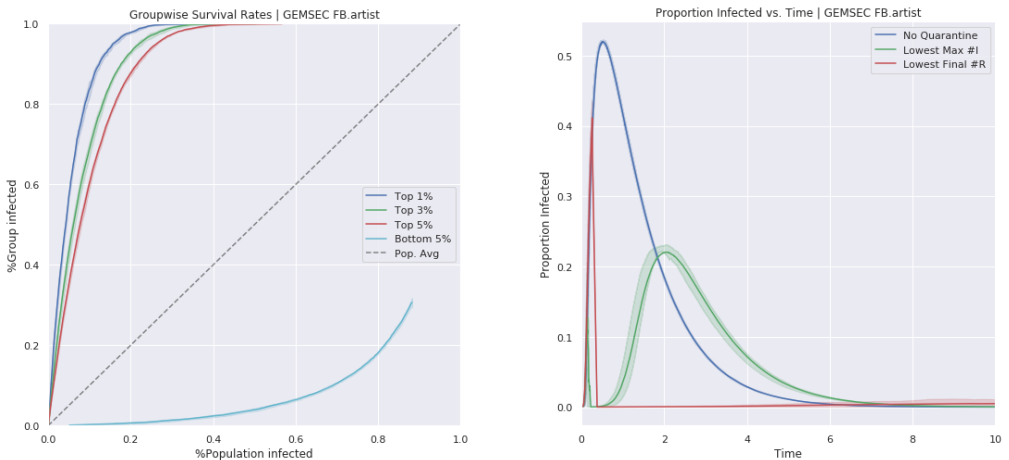


Fig. 1. Experiments run on the GEMSEC Facebook Artist network. On the left, we see groupwise survival rates. Observe that the higher degree nodes become Infected much more quickly than the population average. On the right, we observe the proportion of simultaneously Infected population versus time. The Blue curves indicate the no quarantine setting; the green curves minimize the peak height, whereas the red curves minimize the total number of Infected nodes.

dotted line corresponds to the case where the group considered is the entire population. Curves that lie above the dotted line indicate groups that are Infected more rapidly than average nodes. We plot a similar result for a synthetic BA graph with ($m = 10$) in the appendix. We remark that the considered Facebook graph is even starker than the BA graph, suggesting that this effect is stronger in real networks than some of the synthetic networks considered.

4.3 Single Quarantine Results

We first present results when only a single quarantine was enacted. Throughout we focus our attention on the GEMSEC Facebook Artist network, a real-life network. Most experiments are also conducted on Barabasi-Albert networks with parameter $m = 10$, and can be found on the Appendix. We ultimately demonstrate that the trends exhibited in these networks also are present in the other networks described in Tables 2 and 3.

We outline our single quarantine results. First we demonstrate the curves of the number of Infected nodes versus time to demonstrate the effects of a well-placed quarantine. Then we describe what happens to the total and maximum number of nodes Infected as we vary when the quarantine is enacted, arguing that there are three distinct qualitative quarantine regimes. Next we focus more closely on the structure of a surviving network once an optimally placed quarantine is applied. Then we describe the properties of the second wave of an epidemic that occurs after a quarantine is enacted. Finally we ablate against the infectiousness parameter to demonstrate how a weaker or stronger infection affects the aforementioned results.

4.3.1 Survival Versus Time. We consider the GEMSEC Facebook artist graph. For this network, in Figure 1 (right) we plot the number of nodes currently Infected versus time under three quarantine settings. In blue, we plot the no-quarantine scenario as a baseline. In red we plot the quarantine strategy that minimizes the total number of nodes who become Infected, and in green we plot the quarantine strategy that minimizes the maximum number of nodes who are Infected at any one time. The blue curve describes one potential goal for controlling an epidemic: minimizing the total number of people who ever are Infected by the disease. Whereas the green curve describes another potential goal that gained particular attention in the COVID-19 pandemic: ensuring that the medical system was not overwhelmed at any one time. A similar plot is shown in the Appendix, where we note these curves are qualitatively similar between the real and synthetic networks.

4.3.2 Varying the Quarantine Threshold. Continuing with our primary examples of GEMSEC.fb.artist and BA10 graphs, we plot the total number of nodes who were Infected versus the quarantine threshold in Figure 2. In each plot, the red curve represents the maximum number of simultaneously Infected nodes, whereas the blue curve represents the total number of Infected nodes. We notice three distinct regions along these curves. The first region occurs when the quarantine occurs very early and not enough of the high-degree nodes of the network have been affected. In this case, the second epidemic dominates and the "second wave" has a larger peak. The minimum of the red curve denotes the boundary between the first and second region and corresponds to the situation where the peak-height of the first and second waves are balanced. The second region occurs between the minimum of the red and blue curves and represents the situation where the first wave has a larger peak but the quarantine is effective in reducing the total number of Infected nodes. The optimal number of total Infected nodes is attained at the earliest quarantine that ensures that there is no second wave. This is observable by noticing that the blue curve in the third region is colinear with the identity line: if there were a secondary infection, the blue curve would lie strictly above the identity line. In the right-hand plot of Figure 2 we note that there is a flat region of the blue curve when the quarantine threshold is very high: this is because the epidemic parameters are such that the population is never entirely Infected.

To demonstrate that the trends shown above do not apply only to these archetypal networks, we present the total number of Infected nodes versus quarantine threshold for the entire suite of synthetic and real networks in Figure 3. Notice that each of these networks display the same qualitative features but differ in their height, maximal benefit of quarantine, and location of optimal quarantine threshold.

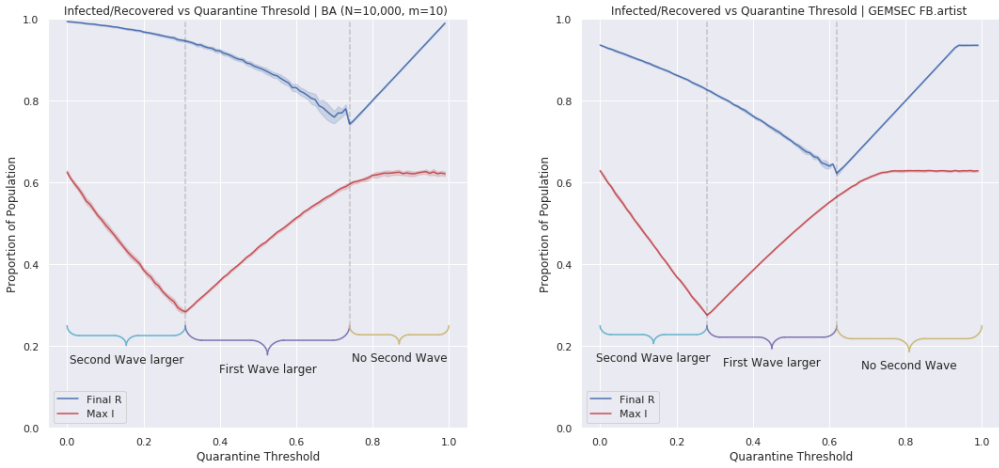


Fig. 2. Proportion of population Infected in total (blue curves), and maximum simultaneously Infected population (red curves) versus the quarantine threshold. The left plot is for the BA network, and the right plot is for the GEMSEC Fb.Artist network. Notice that these graphs are qualitatively similar and there are three distinct regions. In the first region, the quarantine is enacted early and the second wave dominates. In the second region, the quarantine is enacted such that the second wave is larger than the first wave, and in the third region there is no second wave. To minimize the number of Infected nodes in total, there should be no second wave.

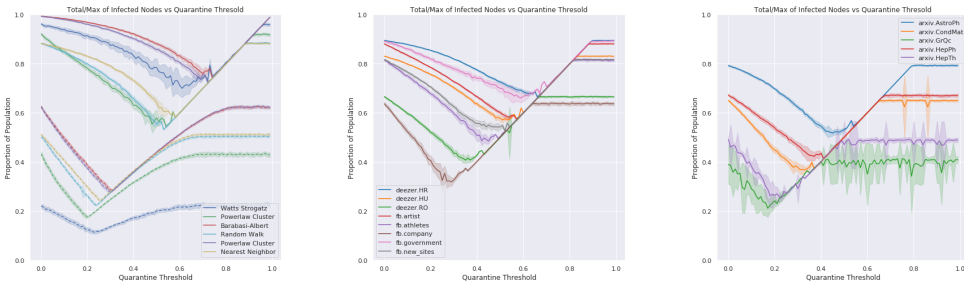


Fig. 3. We plot the same graphs as in Figure 2, for the whole suite of synthetic networks (left), the GEMSEC networks (middle) and the Arxiv Collaboration networks. We only plot the total Infected curves (blue in Figure 2). We note that while varying graphs may have various quarantine strategy and efficacy, the qualitative properties remain.

4.3.3 Structural Changes After a Quarantine. Now we examine the structure of the remaining subgraph after an optimal quarantine has been enacted. In Table 4 we compare various graph metrics between the original network and the network that results after performing the single-quarantine that minimizes the total number of Infected nodes. We consider the average degree and average shortest path. Average shortest path is taken by considering 100,000 random pairs of nodes in the largest connected component and computing their shortest path. We notice that for all synthetic graphs, except Watts Strogatz, the average degree reduces dramatically with the optimal-quarantine networks having degrees between 1 and 2. The shortest paths increase by

Net Type	Params	Deg	Deg'	% Change	S.P.	S.P'	% Change
BA	($m = 5$)	9.99	1.19	-88.10%	3.68	18.58	+405.39%
BA	($m = 10$)	19.98	1.3	-93.51%	3.06	14.92	+388.31%
NN	($u = 0.88, k = 6$)	26.09	1.05	-95.99%	3.41	17.86	+424.43%
PLC	($m = 5, p = 0.5$)	9.99	1.39	-86.13%	3.51	18.12	+416.18%
PLC	($m = 10, p = 0.25$)	19.96	1.29	-93.54%	2.97	13.97	+370.70%
RW	($q_e = 0.91, q_v = 0.94$)	18.95	1.65	-91.29%	3.5	17.65	+404.89%
WS	($k = 10, p = 0.05$)	10	5.09	-49.07%	7.45	11.71	+57.13%

Table 4. Change of summary statistics between generated graphs and the subgraph of susceptible nodes only after an optimal quarantine was performed (denoted with a superscript tick). As noted, an optimal quarantine ensures that no second wave is possible, which the summary statistics reflect: the networks become much sparser and the small-world effect is dampened.

Net Type	Deg	Deg'	% Change	S.P.	S.P'	% Change
arxiv.AstroPh	21.11	3.09	-85.37%	4.17	10.29	+146.43%
arxiv.CondMat	8.08	2.87	-64.53%	5.35	12.41	+131.97%
arxiv.GrQc	5.53	3.23	-41.57%	6.06	10.89	+79.58%
arxiv.HepPh	19.74	2.73	-86.16%	4.67	10.95	+134.59%
arxiv.HepTh	5.26	2.31	-56.19%	5.96	12.6	+111.55%
deezer.HR	18.26	2.02	-88.96%	4.52	10.39	+129.89%
deezer.HU	9.38	2.05	-78.14%	5.33	11.48	+115.21%
deezer.RO	6.02	1.94	-67.85%	6.36	14.46	+127.39%
fb.artist	32.44	1.67	-94.85%	3.69	12.97	+251.16%
fb.athletes	12.53	2.21	-82.39%	4.28	10.4	+142.71%
fb.company	7.41	2.67	-63.93%	5.29	12.82	+142.10%
fb.government	25.35	2.56	-89.92%	3.77	9.99	+164.77%
fb.new_sites	14.78	2.48	-83.23%	4.39	12.93	+194.31%

Table 5. Change of summary statistics between the real networks and their optimal-quarantine subgraphs. On real networks we see the same qualitative effect as the synthetic networks (c.f. Table 4) but to a lesser extent.

a factor of 3-4x, indicating that these networks become much more tree-like and have a lesser small-world-effect, thus it is no surprise that a second wave cannot occur. In table 5 we show similar results for real networks. This indicates that the reductions in average degree and increase in shortest path length under an optimal quarantine are present in a realistic setting as well, albeit to not so drastic an extent.

4.3.4 Characterizing the secondary infection. If a quarantine is enacted before herd immunity is reached, there will be a second "wave" of the epidemic upon reinfection. In Figure 4 (left), we plot the probability that second wave occurs at all, versus the quarantine threshold. We define a second wave occurring as the event that at least 5% of remaining nodes after a quarantine become Infected. Notice that there is a sharp threshold for which a second wave becomes impossible as the quarantine proceeds, and after the optimal quarantine threshold, no second wave occurs at all, which means this quarantine threshold guarantees herd immunity. In Figure 4 (right), we plot the width of the second wave relative to the width of the no-quarantine setting. Width is calculated as the full-width at half-maximum. We observe that the second wave becomes wider as we increase

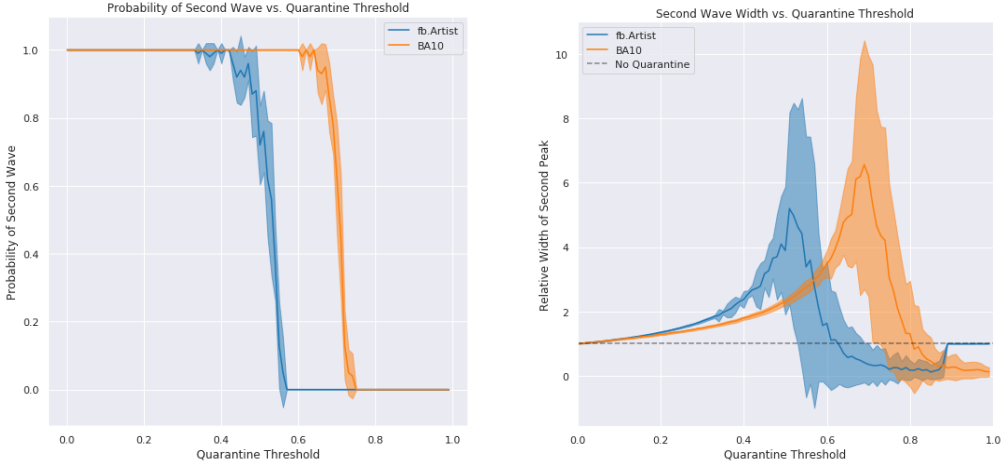


Fig. 4. We plot the probability of a second wave occurring for the BA network and GEMSEC Facebook Artist network (left). Observe that there is a sharp dropoff as the quarantine threshold approaches the optimal. On the right, we plot the FWHM width of the second peak relative to the width of the infection curve in the no-quarantine setting. Even when suboptimal quarantines are enacted, the second wave becomes wider.

the quarantine threshold, indicating that it takes longer for the infection to propagate through the population, even if the quarantine is enacted suboptimally.

Weaker and Stronger infections. Until now, we have rather arbitrarily selected the ratio of infection to recovery parameters, $\frac{\beta}{\gamma}$ to be 0.5, such that the entire population becomes Infected if no quarantine is enacted. To clarify that the empirical phenomena we have discussed are not particular to this setting of infection, and to describe the effect of a stronger and weaker infection, we have run all of our simulations under the same setting where the infection parameter is varied between $\{\frac{1}{32}, \frac{1}{16}, \frac{1}{8}, \frac{1}{4}, \frac{1}{2}, 1, 2, 4, 8, 16, 32\}$. In Figure 5 we plot the total number of Infected nodes for these varying ratios. We note that for exceptionally weak epidemics, the data is very noisy and essentially flat, indicating that epidemics are very unlikely to propagate at all. Next we observe that as an infection becomes stronger, in the sense that $\frac{\beta}{\gamma}$ is larger, the optimal quarantine threshold is higher and the quarantine is less effective. Indeed, for comparatively stronger epidemics, the trough in each V-shaped curve is shallower and further to the right. We posit that this is because the chance of the infection propagating along any single edge is much greater for strong epidemics and thus everyone becomes Infected even networks with extremely light-tailed degree distributions. Hence, even when the high-degree nodes quickly become eradicated early during the course of the epidemic, the remaining susceptible subnetwork will allow every node to become Infected, regardless of where the quarantine is applied.

4.3.5 Clustering and Nodes. Our theoretical results have been established in the configuration model, when networks are infinite and the clustering coefficient is vanishing. By varying the size of the network and the clustering coefficient, we prove those assumption have negligible impact on the final fraction of Removed nodes. See Appendix for exact plots.

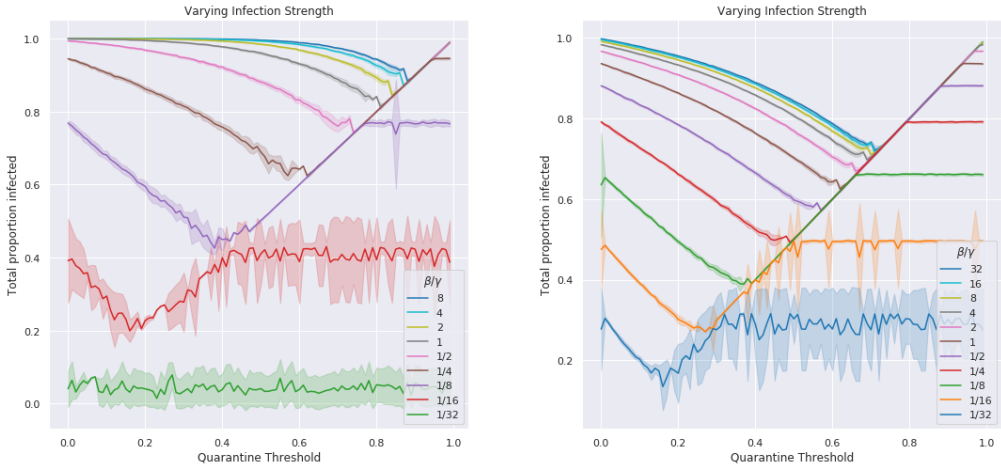


Fig. 5. We ablate across the infection parameters β/γ for the BA network (left) and GEMSEC Facebook Artist network (right) by plotting the total proportion of population Infected versus quarantine threshold. The qualitative properties do not change as the infection parameters are varied, though weaker infections have an optimal quarantine threshold that is earlier than a stronger infection.

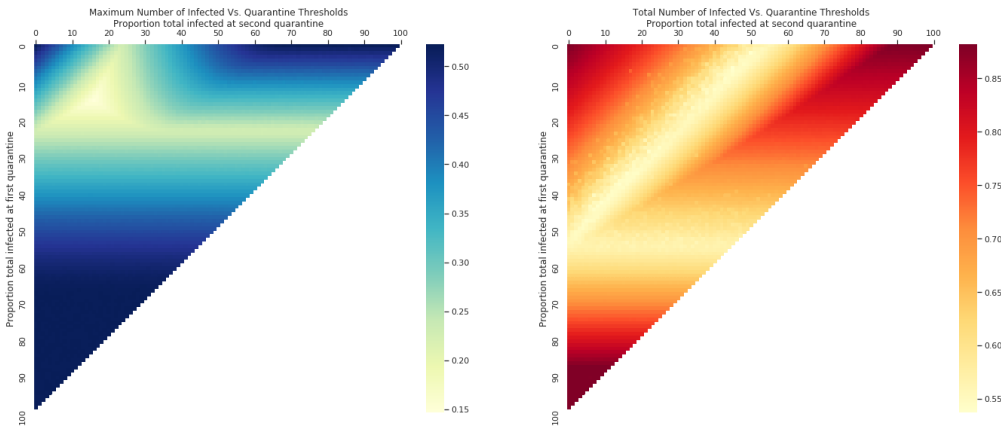


Fig. 6. Effect of two quarantines on the GEMSEC Facebook Artist network. The left plot displays maximum number of Infected nodes, and the right plot displays the total number of Infected nodes. The vertical axis corresponds to the proportion of the population who has been Infected at the time of first quarantine. The horizontal axis corresponds to second quarantine threshold, in terms of the proportion of the (total) population who has been Infected since the first quarantine. Observe that there is an optimal strategy in the two-quarantine setting that does better than the single-quarantine setting for the maximum Infected nodes, whereas it is in general impossible to do better than the single quarantine setting for minimizing total number of Infected nodes.

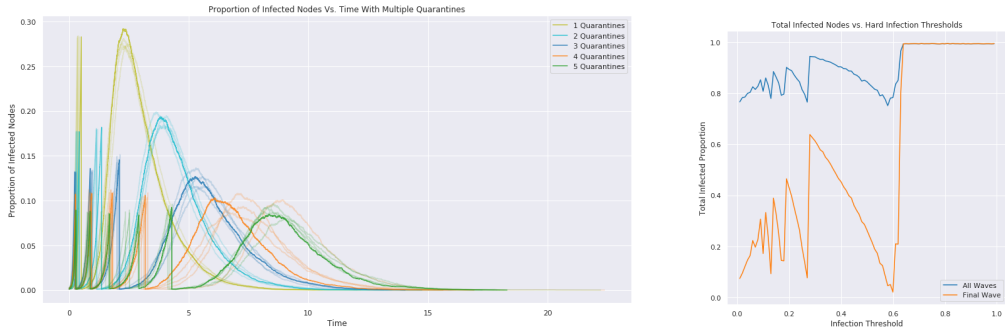


Fig. 7. In the left plot, we map plot the number of Infected nodes versus time when multiple quarantines are allowed. The quarantine strategy is chosen to keep peak heights roughly equal. Notice that the final peaks get wider and there is diminishing returns in peak reduction as quarantines are increased. On the right, we plot the total number of Infected nodes when a hard infection threshold is enacted. Notice that the final number of nodes Infected is greatly dependent upon the number of nodes Infected by the final wave, and the optimal situation is to have an impotent final wave.

4.4 Multiple Quarantines

4.4.1 Two Quarantines. We examine the effects of performing two quarantines. We plot these results for the GEMSEC Facebook Artist graphs in Figure 6 (see Appendix for similar result on Barabasi-Albert graphs). A two-quarantine simulation is run in a similar fashion to a single-quarantine simulation, where the second quarantine threshold refers to the proportion of the original network that becomes Infected between the first and second quarantine. The heatmaps in Figure 6 display the first quarantine threshold on the vertical axis and the second quarantine threshold on the horizontal axis, thereby recovering the V-plots of Figure 2 in either the left column or the top row of the heatmaps. From there, we can conclude that having two quarantines can reduce the maximum number of Infected nodes, but not the Total number of Infected nodes. On one hand, this is disappointing, as we cannot reduce the final number of Removed nodes $R(u)$ by using more quarantines. On the other hand, this means that if we need to declare a quarantine earlier than at the optimal time, say because of a constraint on the maximum number of simultaneously Infected nodes (e.g. hospital beds), we can recover all the benefits of a single well-timed quarantine with two well-timed quarantines. We now extend this observation to more than two quarantines.

4.4.2 More than two quarantines. Finally we turn our attention to the case when more than two quarantines are applied. In Figure 7 (left) we plot the proportion of Infected nodes versus time for the BA10 graph under various scenarios with multiple quarantines. The quarantine thresholds are chosen to roughly equalize the peak heights. Naturally we notice that the peak heights decay as we increase the number of quarantines we're allowed, however the improvement in peak height has diminishing returns. We also notice that the latter peaks are wider than the initial peaks, echoing our observation in the single-quarantine setting.

In Figure 7 (right), instead of declaring a quarantine based on the fraction of nodes not in the Susceptible state, we declare it when the number of nodes in the Infected state reaches a certain threshold, and then restart a new infection after each quarantine. We then plot the final number of Removed nodes after these multiple quarantines. Notice that this strategy does not need any knowledge of the graph (not even the degree sequence). A multiple value of the threshold allow us to recover the result of a well-timed single quarantine. However, if the threshold is poorly chosen,

the final number of Removed nodes can be multiple times greater than the optimal achievable. The higher the threshold, the worse this strategy can behave. Nevertheless, if quarantines are declared early (when a small fraction of the population is Infected), we are always within a factor 2 of the optimal number of nodes in the Removed state. Multiple quarantines can therefore be used as a targeted immunization strategy even without any knowledge of the contact graph, as long as they are declared early.

REFERENCES

- [1] Bruno Abrahao, Flavio Chierichetti, Robert Kleinberg, and Alessandro Panconesi. 2013. Trace complexity of network inference. *Proceedings of the 19th ACM SIGKDD international conference on Knowledge discovery and data mining - KDD '13* (2013), 491. <https://doi.org/10.1145/2487575.2487664> arXiv:arXiv:1308.2954v1
- [2] Md Manjurul Ahsan, Kishor Datta Gupta, Mohammad Maminur Islam, Sajib Sen, Md. Lutfar Rahman, and Mohammad Shakhawat Hossain. 2020. Study of Different Deep Learning Approach with Explainable AI for Screening Patients with COVID-19 Symptoms: Using CT Scan and Chest X-ray Image Dataset. arXiv:2007.12525 [eess.IV]
- [3] William Aiello, Fan Chung, and Linyuan Lu. 2000. A random graph model for massive graphs. In *Proceedings of the thirty-second annual ACM symposium on Theory of computing*. 171–180.
- [4] William Aiello, Fan Chung, and Linyuan Lu. 2002. Random evolution in massive graphs. In *Handbook of massive data sets*. Springer, 97–122.
- [5] Firoj Alam, Fahim Dalvi, Shaden Shaar, Nadir Durrani, Hamdy Mubarak, Alex Nikolov, Giovanni Da San Martino, Ahmed Abdelali, Hassan Sajjad, Kareem Darwish, and Preslav Nakov. 2020. Fighting the COVID-19 Infodemic in Social Media: A Holistic Perspective and a Call to Arms. arXiv:2007.07996 [cs.IR]
- [6] Réka Albert, Hawoong Jeong, and Albert-László Barabási. 2000. Error and attack tolerance of complex networks. *nature* 406, 6794 (2000), 378–382.
- [7] Luis A Nunes Amaral, Antonio Scala, Marc Barthélemy, and H Eugene Stanley. 2000. Classes of small-world networks. *Proceedings of the national academy of sciences* 97, 21 (2000), 11149–11152.
- [8] Ery Arias-Castro, Emmanuel J Candès, and Arnaud Durand. 2011. Detection of an anomalous cluster in a network. *The Annals of Statistics* 39, 1 (2011), 278–304. <https://doi.org/10.1214/10-AOS839> arXiv:arXiv:1001.3209v2
- [9] Ery Arias-Castro and S T Nov. [n.d.]. Detecting a Path of Correlations in a Network. ([n.d.]), 1–12. arXiv:arXiv:1511.01009v1
- [10] Albert-László Barabási and Réka Albert. 1999. Emergence of scaling in random networks. *science* 286, 5439 (1999), 509–512.
- [11] Lars Baumgärtner, Alexandra Dmitrienko, Bernd Freisleben, Alexander Gruler, Jonas Höchst, Joshua Kühlberg, Mira Mezini, Markus Miettinen, Anel Muhamedagic, Thien Duc Nguyen, Alvar Penning, Dermot Frederik Pustelnik, Filipp Roos, Ahmad-Reza Sadeghi, Michael Schwarz, and Christian Uhl. 2020. Mind the GAP: Security and Privacy Risks of Contact Tracing Apps. arXiv:2006.05914 [cs.CR]
- [12] Caroline O. Buckee, Satchit Balsari, Jennifer Chan, Mercè Crosas, Francesca Dominici, Urs Gasser, Yonatan H. Grad, Bryan Grenfell, M. Elizabeth Halloran, Moritz U. G. Kraemer, Marc Lipsitch, C. Jessica E. Metcalf, Lauren Ancel Meyers, T. Alex Perkins, Mauricio Santillana, Samuel V. Scarpino, Cecile Viboud, Amy Wesolowski, and Andrew Schroeder. 2020. Aggregated mobility data could help fight COVID-19. *Science* 368, 6487 (2020), 145–146. <https://doi.org/10.1126/science.abb8021> arXiv:https://science.sciencemag.org/content/368/6487/145.2.full.pdf
- [13] Camila Buono and Lidia A Braunstein. 2015. Immunization strategy for epidemic spreading on multilayer networks. *EPL (Europhysics Letters)* 109, 2 (2015), 26001.
- [14] Justin Chan, Dean Foster, Shyam Gollakota, Eric Horvitz, Joseph Jaeger, Sham Kakade, Tadayoshi Kohno, John Langford, Jonathan Larson, Puneet Sharma, Sudheesh Singanamalla, Jacob Sunshine, and Stefano Tessaro. 2020. PACT: Privacy Sensitive Protocols and Mechanisms for Mobile Contact Tracing. arXiv:2004.03544 [cs.CR]
- [15] Qian Chen, Hyunseok Chang, Ramesh Govindan, and Sugih Jamin. 2002. The origin of power laws in Internet topologies revisited. In *Proceedings. twenty-first annual joint conference of the ieee computer and communications societies*, Vol. 2. IEEE, 608–617.
- [16] Yiping Chen, Gerald Paul, Shlomo Havlin, Fredrik Liljeros, and H Eugene Stanley. 2008. Finding a better immunization strategy. *Physical review letters* 101, 5 (2008), 058701.
- [17] Justin Cheng, Lada A. Adamic, P. Alex Dow, Jon Kleinberg, and Jure Leskovec. 2014. Can Cascades be Predicted?. In *Proceedings of the 23rd international conference on World wide web (WWW' 14)*. <https://doi.org/10.1145/2566486.2567997> arXiv:1403.4608
- [18] Reuven Cohen, Shlomo Havlin, and Daniel Ben-Avraham. 2003. Efficient immunization strategies for computer networks and populations. *Physical review letters* 91, 24 (2003), 247901.
- [19] Hadi Daneshmand, Manuel Gomez-Rodriguez, Le Song, and Bernhard Schoelkopf. 2014. Estimating Diffusion Network Structures: Recovery Conditions, Sample Complexity & Soft-thresholding Algorithm. In *Proceedings of the 31 st International Conference on Machine Learning, Beijing, China, 2014 - ICML 14*. <https://doi.org/10.1002/aur.1474>. Replication arXiv:1405.2936
- [20] Michela Del Vicario, Alessandro Bessi, Fabiana Zollo, Fabio Petroni, Antonio Scala, Guido Caldarelli, H. Eugene Stanley, and Walter Quattrociocchi. 2016. The spreading of misinformation online. *Proceedings of the National Academy of Sciences* (2016), 201517441. <https://doi.org/10.1073/pnas.1517441113>
- [21] Ming Dong, Bolong Zheng, Nguyen Quoc Viet Hung, Han Su, and Guohui Li. 2019. Multiple Rumor Source Detection with Graph Convolutional Networks. In *Proceedings of the 28th ACM International Conference on Information and*

Knowledge Management. 569–578.

- [22] Kimon Drakopoulos, Asuman Ozdaglar, and John N. Tsitsiklis. 2014. An efficient curing policy for epidemics on graphs. *arXiv preprint arXiv:1407.2241* December (2014), 1–10. <https://doi.org/10.1109/TNSE.2015.2393291> arXiv:arXiv:1407.2241v1
- [23] Kimon Drakopoulos, Asuman Ozdaglar, and John N. Tsitsiklis. 2015. A lower bound on the performance of dynamic curing policies for epidemics on graphs. 978 (2015), 3560–3567. <https://doi.org/10.1109/CDC.2015.7402770> arXiv:1510.06055
- [24] Zhanwei Du, Lin Wang, Simon Cauchemez, Xiaoke Xu, Xianwen Wang, Benjamin J Cowling, and Lauren Ancel Meyers. 2020. Risk for transportation of coronavirus disease from Wuhan to other cities in China. *Emerging infectious diseases* 26, 5 (2020), 1049.
- [25] Daniel Duque, David Paul Morton, Bismark Singh, Zhanwei Du, Remy Pasco, and Lauren Ancel Meyers. 2020. COVID-19: How to Relax Social Distancing If You Must. *medRxiv* (2020). <https://doi.org/10.1101/2020.04.29.20085134> arXiv:<https://www.medrxiv.org/content/early/2020/05/05/2020.04.29.20085134.full.pdf>
- [26] Daniel Duque, David P. Morton, Bismark Singh, Zhanwei Du, Remy Pasco, and Lauren Ancel Meyers. 2020. Timing social distancing to avert unmanageable COVID-19 hospital surges. *Proceedings of the National Academy of Sciences* (2020). <https://doi.org/10.1073/pnas.2009033117> arXiv:<https://www.pnas.org/content/early/2020/07/28/2009033117.full.pdf>
- [27] Giulia Fanti, Peter Kairouz, Sewoong Oh, Kannan Ramchandran, and Pramod Viswanath. 2016. Rumor source obfuscation on irregular trees. In *Proceedings of the 2016 ACM SIGMETRICS International Conference on Measurement and Modeling of Computer Science (SIGMETRICS' 16)*. ACM, 153–164.
- [28] Giulia Fanti, Peter Kairouz, Sewoong Oh, Kannan Ramchandran, and Pramod Viswanath. 2017. Hiding the Rumor Source. *IEEE Transactions on Information Theory* 63, 10 (2017), 6679–6713. <https://doi.org/10.1109/TIT.2017.2696960> arXiv:1509.02849
- [29] Giulia Fanti, Peter Kairouz, Sewoong Oh, and Pramod Viswanath. 2015. Spy vs. Spy: Rumor Source Obfuscation. *Proceedings of the 2015 ACM SIGMETRICS International Conference on Measurement and Modeling of Computer Systems (SIGMETRICS' 14)* (2015), 271–284. <https://doi.org/10.1145/2745844.2745866> arXiv:1412.8439
- [30] Mehrdad Farajtabar, Jiachen Yang, Xiaojing Ye, Huan Xu, Rakshit Trivedi, Elias Khalil, Shuang Li, Le Song, and Hongyuan Zha. 2017. Fake News Mitigation via Point Process Based Intervention. In *Proceedings of the 34th International Conference on Machine Learning (ICML' 17)*. arXiv:1703.07823 <http://arxiv.org/abs/1703.07823>
- [31] Yuanyuan Feng, Gautam Iyer, and Lei Li. 2020. Scheduling fixed length quarantines to minimize the total number of fatalities during an epidemic. arXiv:2007.09519 [math.DS]
- [32] Spencer J Fox, Remy Pasco, Mauricio Tec, Zhanwei Du, Michael Lachmann, James Scott, and Lauren Ancel Meyers. 2020. The impact of asymptomatic COVID-19 infections on future pandemic waves. *medRxiv* (2020). <https://doi.org/10.1101/2020.06.22.20137489> arXiv:<https://www.medrxiv.org/content/early/2020/06/23/2020.06.22.20137489.full.pdf>
- [33] Manuel Gomez-Rodriguez, Jure Leskovec, and Bernhard Schölkopf. 2013. Structure and Dynamics of Information Pathways in Online Media. In *6th International Conference on Web Search and Data Mining (WSDM 2013)*.
- [34] Jessica Hoffmann, Soumya Basu, Surbhi Goel, and Constantine Caramanis. 2019. Learning Mixtures of Graphs from Epidemics Cascades. *CoRR* abs/1906.06057 (2019). arXiv:1906.06057 <http://arxiv.org/abs/1906.06057>
- [35] Jessica Hoffmann and Constantine Caramanis. 2018. The Cost of Uncertainty in Curing Epidemics. *Proceedings of the ACM on Measurement and Analysis of Computing Systems (SIGMETRICS' 18)* 2, 2 (2018), 11–13. <https://doi.org/10.1145/3219617.3219622>
- [36] Jessica Hoffmann and Constantine Caramanis. 2019. Learning graphs from noisy epidemic cascades. *Proceedings of the ACM on Measurement and Analysis of Computing Systems* 3, 2 (2019), 1–34.
- [37] Petter Holme. 2004. Efficient local strategies for vaccination and network attack. *EPL (Europhysics Letters)* 68, 6 (2004), 908.
- [38] Petter Holme and Beom Jun Kim. 2002. Growing scale-free networks with tunable clustering. *Physical review E* 65, 2 (2002), 026107.
- [39] Ramon Ferrer i Cancho, Christiaan Janssen, and Ricard V Solé. 2001. Topology of technology graphs: Small world patterns in electronic circuits. *Physical Review E* 64, 4 (2001), 046119.
- [40] Hawoong Jeong, Sean P Mason, A-L Barabási, and Zoltan N Oltvai. 2001. Lethality and centrality in protein networks. *Nature* 411, 6833 (2001), 41–42.
- [41] Ioannis Karamouzas, Brian Skinner, and Stephen J. Guy. 2014. Universal Power Law Governing Pedestrian Interactions. *Phys. Rev. Lett.* 113 (Dec 2014), 238701. Issue 23. <https://doi.org/10.1103/PhysRevLett.113.238701>
- [42] Justin Khim and Po-Ling Loh. 2017. Permutation Tests for Infection Graphs. (2017), 1–28. arXiv:1705.07997 <http://arxiv.org/abs/1705.07997>
- [43] Justin Khim and Po-Ling Loh. 2018. A theory of maximum likelihood for weighted infection graphs. (2018), 1–47. arXiv:arXiv:1806.05273v1 <https://arxiv.org/pdf/1806.05273.pdf>

- [44] Jon M Kleinberg. 2002. Small-world phenomena and the dynamics of information. In *Advances in neural information processing systems*. 431–438.
- [45] Naimisha Kolli and Balakrishnan Narayanaswamy. 2019. Influence Maximization From Cascade Information Traces in Complex Networks in the Absence of Network Structure. *IEEE Transactions on Computational Social Systems* 6, 6 (2019), 1147–1155.
- [46] Jure Leskovec, Jon Kleinberg, and Christos Faloutsos. 2007. Graph evolution: Densification and shrinking diameters. *ACM transactions on Knowledge Discovery from Data (TKDD)* 1, 1 (2007), 2–es.
- [47] Jure Leskovec, Andreas Krause, Carlos Guestrin, Christos Faloutsos, Jeanne VanBriesen, and Natalie Glance. 2007. Cost-effective Outbreak Detection in Networks. *Proceedings of the 13th ACM SIGKDD international conference on Knowledge discovery and data mining (KDD '07)* (2007), 420. <https://doi.org/10.1145/1281192.1281239>
- [48] Jure Leskovec and Andrej Krevl. 2014. SNAP Datasets: Stanford Large Network Dataset Collection. <http://snap.stanford.edu/data>.
- [49] Fredrik Liljeros, Christofer R Edling, and Luis A Nunes Amaral. 2003. Sexual networks: implications for the transmission of sexually transmitted infections. *Microbes and infection* 5, 2 (2003), 189–196.
- [50] Fredrik Liljeros, Christofer R Edling, Luis A Nunes Amaral, H Eugene Stanley, and Yvonne Åberg. 2001. The web of human sexual contacts. *Nature* 411, 6840 (2001), 907–908.
- [51] Shenghua Liu, Huawei Shen, Houdong Zheng, Xueqi Cheng, and Xiangwen Liao. 2019. CT LIS: Learning Influences and Susceptibilities through Temporal Behaviors. *ACM Transactions on Knowledge Discovery from Data (TKDD)* 13, 6 (2019), 1–21.
- [52] Lars Lorch, William Trouleau, Stratis Tsirtsis, Aron Szanto, Bernhard Schölkopf, and Manuel Gomez-Rodriguez. 2020. A Spatiotemporal Epidemic Model to Quantify the Effects of Contact Tracing, Testing, and Containment. arXiv:2004.07641 [cs.LG]
- [53] Tania Martin, Georgios Karopoulos, José L. Hernández-Ramos, Georgios Kambourakis, and Igor Nai Fovino. 2020. Demystifying COVID-19 digital contact tracing: A survey on frameworks and mobile apps. arXiv:2007.11687 [cs.CR]
- [54] Atalanti Mastakouri and Bernhard Schölkopf. 2020. Causal analysis of Covid-19 spread in Germany. *Advances in Neural Information Processing Systems* 33 (2020).
- [55] Rosemary M McCloskey, Richard H Liang, and Art FY Poon. 2016. Reconstructing contact network parameters from viral phylogenies. *Virus evolution* 2, 2 (2016).
- [56] Eli A. Meiron, Chris Milling, Constantine Caramanis, Shie Mannor, Ariel Orda, and Sanjay Shakkottai. 2014. Localized epidemic detection in networks with overwhelming noise. (2014), 1–27. arXiv:1402.1263 <http://arxiv.org/abs/1402.1263>
- [57] Joel C. Miller and Tony Ting. 2019. EoN (Epidemics on Networks): a fast, flexible Python package for simulation, analytic approximation, and analysis of epidemics on networks. *Journal of Open Source Software* 4, 44 (2019), 1731. <https://doi.org/10.21105/joss.01731>
- [58] Chris Milling, Constantine Caramanis, Shie Mannor, and Sanjay Shakkottai. 2012. Network Forensics : Random Infection vs Spreading Epidemic. In *Proceedings of the 12th ACM SIGMETRICS/PERFORMANCE joint international conference on Measurement and Modeling of Computer Systems (SIGMETRICS' 12)*.
- [59] Chris Milling, Constantine Caramanis, Shie Mannor, and Sanjay Shakkottai. 2015. Local detection of infections in heterogeneous networks. *Proceedings - IEEE INFOCOM* 26 (2015), 1517–1525. <https://doi.org/10.1109/INFOCOM.2015.7218530>
- [60] Preslav Nakov. 2020. Can We Spot the "Fake News" Before It Was Even Written? arXiv:2008.04374 [cs.CL]
- [61] Praneeth Netrapalli and Sujay Sanghavi. 2012. Learning the Graph of Epidemic Cascades. In *Proceedings of the 12th ACM SIGMETRICS/PERFORMANCE joint international conference on Measurement and Modeling of Computer Systems (SIGMETRICS' 12)*. 211–222. <https://doi.org/10.1145/2318857.2254783> arXiv:1202.1779
- [62] Mark Newman. 2018. *Networks*. Oxford university press.
- [63] Han-Ching Ou, Arunesh Sinha, Sze-Chuan Suen, Andrew Perrault, and Milind Tambe. 2019. Who and When to Screen: Multi-Round Active Screening for Recurrent Infectious Diseases Under Uncertainty. arXiv:1903.06113 [q-bio.QM]
- [64] Bastien Pasdeloup, Vincent Gripon, Grégoire Mercier, Dominique Pastor, and Michael G Rabbat. 2017. Characterization and inference of graph diffusion processes from observations of stationary signals. *IEEE transactions on Signal and Information Processing over Networks* 4, 3 (2017), 481–496.
- [65] Liudmila Prokhorenkova, Alexey Tikhonov, and Nelly Litvak. 2019. Learning clusters through information diffusion. In *The World Wide Web Conference*. 3151–3157.
- [66] Benedek Rozemberczki, Ryan Davies, Rik Sarkar, and Charles Sutton. 2019. Gemsec: Graph embedding with self clustering. In *Proceedings of the 2019 IEEE/ACM international conference on advances in social networks analysis and mining*. 65–72.
- [67] Alessandra Sala, Lili Cao, Christo Wilson, Robert Zablit, Haitao Zheng, and Ben Y Zhao. 2010. Measurement-calibrated graph models for social network experiments. In *Proceedings of the 19th international conference on World wide web*. 861–870.

- [68] Marcel Salathé, Maria Kazandjieva, Jung Woo Lee, Philip Levis, Marcus W. Feldman, and James H. Jones. 2010. A high-resolution human contact network for infectious disease transmission. *Proceedings of the National Academy of Sciences* 107, 51 (2010), 22020–22025. <https://doi.org/10.1073/pnas.1009094108> arXiv:<https://www.pnas.org/content/107/51/22020.full.pdf>
- [69] Christian M Schneider, Tamara Mihaljev, and Hans J Herrmann. 2012. Inverse targeting—An effective immunization strategy. *EPL (Europhysics Letters)* 98, 4 (2012), 46002.
- [70] Parongama Sen, Subinay Dasgupta, Arnab Chatterjee, PA Sreeram, G Mukherjee, and SS Manna. 2003. Small-world properties of the Indian railway network. *Physical Review E* 67, 3 (2003), 036106.
- [71] Devavrat Shah and Tauhid Zaman. 2010. Detecting sources of computer viruses in networks: theory and experiment. In *ACM SIGMETRICS Performance Evaluation Review*, Vol. 38. ACM, 203–214.
- [72] Devavrat Shah and Tauhid Zaman. 2010. Rumors in a Network : Who ' s the Culprit ? *IEEE Transactions on information theory* 57, 8 (2010), 1–43. <https://doi.org/10.1109/TIT.2011.2158885> arXiv:0909.4370
- [73] Devavrat Shah and Tauhid Zaman. 2012. Rumor centrality: a universal source detector. In *ACM SIGMETRICS Performance Evaluation Review*, Vol. 40. ACM, 199–210.
- [74] Afshin Shoeibi, Marjane Khodatars, Roohallah Alizadehsani, Navid Ghassemi, Mahboobeh Jafari, Parisa Moridian, Ali Khadem, Delaram Sadeghi, Sadiq Hussain, Assef Zare, Zahra Alizadeh Sani, Javad Bazeli, Fahime Khozeimeh, Abbas Khosravi, Saeid Nahavandi, U. Rajendra Acharya, and Peng Shi. 2020. Automated Detection and Forecasting of COVID-19 using Deep Learning Techniques: A Review. arXiv:2007.10785 [cs.LG]
- [75] Lucas P. Soares and Cesar P. Soares. 2020. Automatic Detection of COVID-19 Cases on X-ray images Using Convolutional Neural Networks. arXiv:2007.05494 [eess.IV]
- [76] Sam Spencer and R Srikant. 2015. On the impossibility of localizing multiple rumor sources in a line graph. *ACM SIGMETRICS Performance Evaluation Review* 43, 2 (2015), 66–68.
- [77] Anirudh Sridhar and H Vincent Poor. 2019. Sequential Estimation of Network Cascades. *arXiv preprint arXiv:1912.03800* (2019).
- [78] Alexei Vázquez. 2003. Growing network with local rules: Preferential attachment, clustering hierarchy, and degree correlations. *Physical Review E* 67, 5 (2003), 056104.
- [79] Shengling Wang, Shasha Chen, Xiuzhen Cheng, Weifeng Lv, and Jiguo Yu. 2019. Analysis of Antagonistic Dynamics for Rumor Propagation. In *2019 IEEE 39th International Conference on Distributed Computing Systems (ICDCS)*. IEEE, 1253–1263.
- [80] Zhaoxu Wang, Wenxiang Dong, Wenyi Zhang, and Chee Wei Tan. 2014. Rumor source detection with multiple observations: Fundamental limits and algorithms. In *ACM SIGMETRICS Performance Evaluation Review*, Vol. 42. ACM, 1–13.
- [81] Duncan J Watts and Steven H Strogatz. 1998. Collective dynamics of 'small-world' networks. *nature* 393, 6684 (1998), 440–442.
- [82] JG White, E Southgate, JN Thomson, and S Brenner. 1986. The structure of the nervous system of the nematode *Caenorhabditis elegans*. *Philosophical transactions of the Royal Society of London. Series B, Biological sciences* 314, 1165 (1986), 1–340.
- [83] Liang Wu and Huan Liu. 2018. Tracing Fake-News Footprints: Characterizing Social Media Messages by How They Propagate. In *(WSDM 2018) The 11th ACM International Conference on Web Search and Data Mining*. <https://doi.org/10.1145/3159652.3159677>
- [84] Yujia Xie, Haoming Jiang, Feng Liu, Tuo Zhao, and Hongyuan Zha. 2019. Meta Learning with Relational Information for Short Sequences. In *Advances in Neural Information Processing Systems*. 9901–9912.
- [85] Wen Yan, Po-Ling Loh, Chunguo Li, Yongming Huang, and Luxi Yang. 2019. Conquering the Worst Case of Infections in Networks. *IEEE Access* (2019).
- [86] Qingyuan Zhao, Murat A. Erdogdu, Hera Y. He, Anand Rajaraman, and Jure Leskovec. 2015. SEISMIC: A Self-Exciting Point Process Model for Predicting Tweet Popularity. *Proceedings of the 21th ACM SIGKDD International Conference on Knowledge Discovery and Data Mining (KDD '15)* (2015). <https://doi.org/10.1145/2783258.2783401> arXiv:1506.02594

A APPENDIX

A.1 d -regular graphs cannot be immunized through quarantines

PROPOSITION 5. For random d -regular graphs in the configuration model, i.e. with $p_d = 1$ and for $k \neq d, p_k = 0$, it is possible to achieve herd immunity after one quarantine for $d > 2$.

PROOF. For random d -regular graphs in the configuration model, we have:

$$g_0(x) = x^d.$$

Using Claim 5, we need to declare a quarantine when the fraction of nodes of degree 1 u is such that:

$$\begin{aligned} 0 &\geq u^2 g_0''(u) - u g_0'(u) \\ &= u^2 d(d-1)u^{d-2} - u d u^{d-1} \\ &= u^d d(d-2). \end{aligned}$$

This inequality cannot be satisfied for $k > 2$, so quarantining is not a valid immunization strategy. \square

A.2 BA graphs

We first compare groupwise survival rates for BA graphs and a social network, then the proportion of simultaneously Infected nodes versus time. The behavior is similar for both networks.

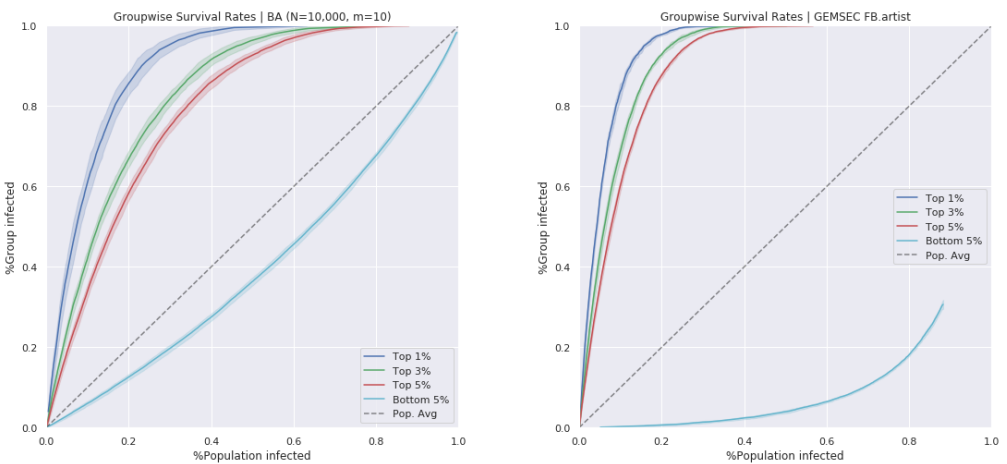


Fig. 8. Groupwise survival rates for a BA graph (left) and a social network (right). Observe that the higher degree nodes become Infected much more quickly than the population average.

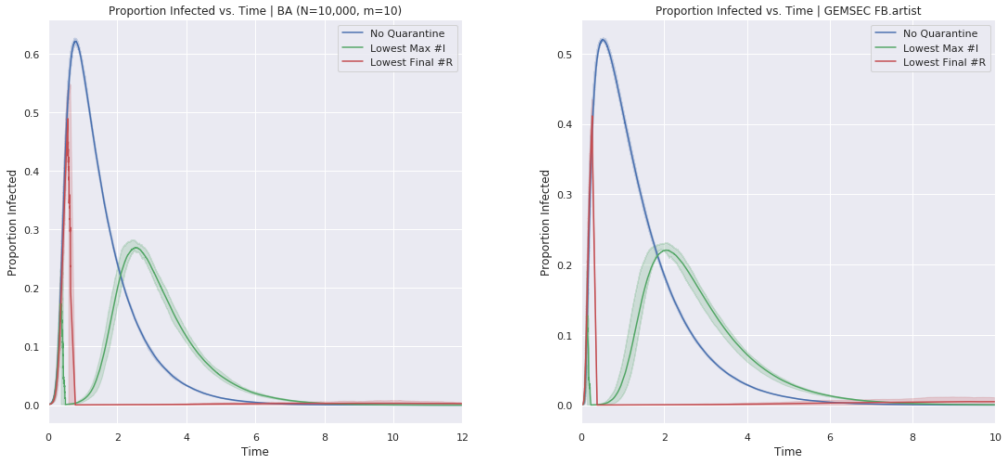


Fig. 9. Proportion of simultaneously Infected population versus time for a BA network with parameter $m = 10$ (left) and the GEMSEC Facebook Artist network (right). The Blue curves indicate the no quarantine setting; the green curves minimize the peak height, whereas the red curves minimize the total number of Infected nodes.

The behavior of a double quarantine is also very similar to the behavior on the GEMSEC Facebook Artist network.

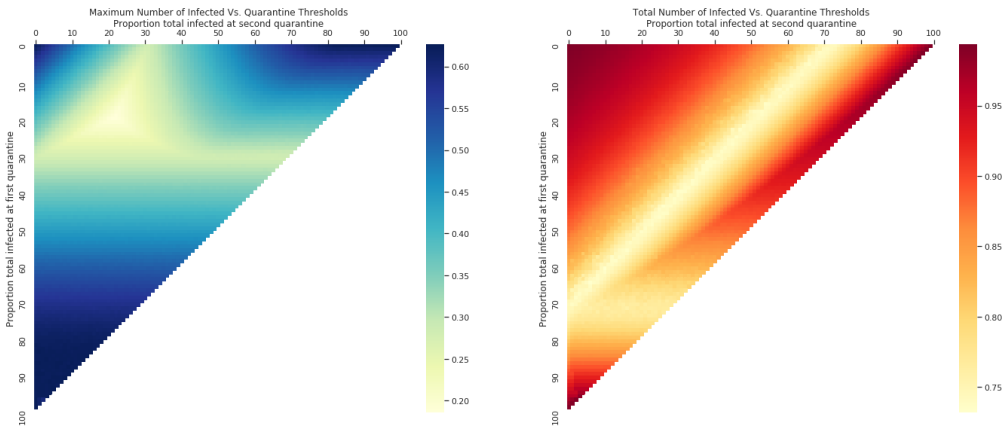


Fig. 10. Effect of two quarantines on the BA graph. Effects are similar to the GEMSEC Facebook Artist graphs.

A.3 Relaxing theoretical assumptions

Even though our theoretical results have been established in for infinite graphs with vanishing clustering coefficient, our empirical results hold for finite networks, and we demonstrate empirically that modifying the clustering coefficient doesn't have a noticeable effect on quarantine efficacy. In Figure 11 (left), we plot the total number of Infected nodes versus quarantine thresholds for a series of PLC networks, where we alter only the parameter p which controls the clustering coefficient. In

Figure 11 (right), we consider a series of BA networks with the same parameter m , but differing sizes. In both cases we notice that the differences across either series are negligible, indicating that the qualitative results we've empirically demonstrated do not depend upon the clustering coefficient or size of the network.

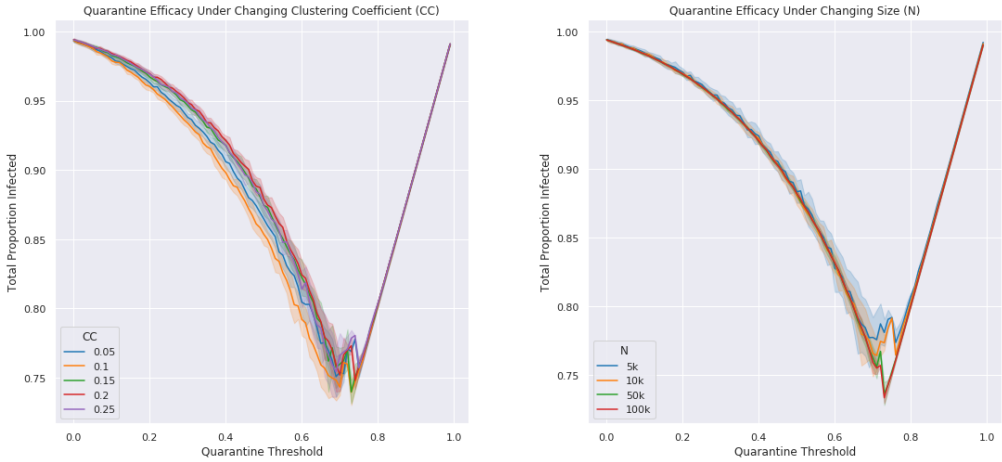


Fig. 11. The effect of quarantines does not depend upon clustering coefficient or size of the network.